Intelligent Driving with Optimal Trajectory Prediction Model for Improved Traffic Flow at Signalized Intersections

Magzhan Atykhan[1], A. S. M. Bakibillah[2], Md Abdus Samad Kamal[1]*, Kou Yamada[1]

[1] Graduate School of Science and Technology, Gunma University, 376-8515 Kiryu, Japan

[2] Department of Systems and Control Engineering, School of Engineering, Institute of Science Tokyo, 152-8552 Tokyo, Japan

* Correspondence: Md Abdus Samad Kamal (maskamal@gunma-u.ac.jp)

Abstract: Effective traffic management at signalized intersections is crucial for enhancing fuel efficiency, safety, and mobility; however, this is challenging for human drivers due to a lack of predictability. This paper proposes a predictive vehicle control system that extends a traditional human-based driving model to optimize traffic flow, reduce intersection transit time, and fuel consumption. The proposed system utilizes an optimal trajectory prediction model to determine the stopping velocity pattern at traffic signals and employs safety gap synchronization, thereby exhibiting human-like car-following behavior. Specifically, the optimal velocity profiles are generated based on a trajectory optimization model over a long-time horizon. A polynomial function is fitted with these optimal trajectories to find the ideal stopping pattern. Instead of repeating the optimization at each step, as in the Model Predictive Control (MPC) approach, our method determines the control acceleration with necessary adjustments while ensuring driving safety. Moreover, the synchronization compensation factor improves the transition from idling to driving conditions. Performance evaluation through microscopic traffic simulations demonstrates improvements in intersection throughput and fuel efficiency, showcasing the effectiveness of the proposed predictive vehicle control system. Unlike the computationally demanding MPC approach, our proposed system offers a practical balance between real-time applicability and traffic flow efficiency.

Keywords: Extended intelligent driver model; Predictive vehicle control; Optimal trajectory prediction; Intersection capacity; Fuel efficiency

1 Introduction

In recent years, Intelligent Transportation Systems (ITS) have demonstrated significant advancements in vehicle automation and traffic management, offering innovative solutions to enhance road capacity, reduce congestion, and improve overall traffic efficiency at signalized intersections [1, 2]. Alternatively, traditional traffic management systems at signalized intersections demonstrate an inadequacy in adaptability to real-time traffic conditions. These issues cause traffic congestion and stop-and-go driving, which leads to increased waiting times, fuel consumption, and greenhouse gas (GHG) emissions [3]. Additionally, existing traffic control systems do not consider the dynamic nature of urban traffic along with emergency vehicles and pedestrian crossings, which further contributes to inefficiencies in urban transportation systems [4]. A study shows that stop-and-go traffic results in a 14% increase in energy consumption and GHG emissions compared to vehicles driven at steady speeds [5]. Consequently, effective intersection control remains a significant challenge in current traffic management systems for ensuring both safe and sustainable urban mobility.

Numerous techniques have been studied to optimize traffic flow at signalized intersections. Initial research primarily focused on developing dynamic and adaptive traffic signal controllers and control algorithms based on traffic queue length data [6, 7]. In these control systems, adaptive signal phase and timing (SPaT) is dynamically computed based on real-time traffic information through vehicle-to-vehicle (V2V) and infra-to-vehicle (I2V) communications to improve traffic flow efficiency [8, 9]. However, limitations of SPaT systems include communication delays, system architecture, and complexity of urban traffic dynamics [R1C3], [R2C4] [10, 11]. Specifically, the absence

of widespread V2V and I2V communication networks limits the potential for cooperative control strategies, thus significantly reducing the effectiveness of intersection traffic management. Alternatively, some studies suggest that machine learning-based models and real-time data analytics could solve these limitation [12, 13]. However, the implementation of learning-based models demands extensive data for training, which is often difficult to obtain [R1C3], [R2C4].

Conversely, the performance of the traffic flow can be improved by enhancing vehicle motion control with desired space and time gaps. Nowadays, adaptive cruise control (ACC) is a practically implemented technology that can regulate vehicle speed by responding to the behavior of the preceding vehicle (PV) [14, 15]. ACC schemes have shown effectiveness in highway driving, where traffic is comparatively consistent [16, 17]. However, in urban traffic conditions, the practical application of ACC is limited due to the presence of critical braking zones, especially at signalized intersections [18]. Particularly, in urban settings where short headways are common, ACC faces instabilities, which can lead to traffic fluctuations, increased fuel consumption, and safety threats [R1C3], [R2C4] [19–21]. Consequently, cooperative adaptive cruise control (CACC) systems have been studied to extend ACC functionality by integrating V2V communication that enables short headway driving [22, 23]. However, CACC improves coordinated vehicle movement based on current traffic conditions without predicting future states. Furthermore, the system is highly dependent on communication infrastructure, which limits application in areas where V2V connectivity is restricted or inconsistent [24, 25].

Numerous studies proposed integrating advanced control algorithms, e.g., MPC, into ACC systems, enabling dynamic decision-making [26, 27]. MPC dynamically optimizes a control input, reducing unnecessary acceleration and braking. As a result, adaptability to dynamic traffic conditions can be improved, resulting in smoother and more energy-efficient vehicle operation [28]. However, MPC-based approaches have high computational demands and limited practical applications. Recent efforts have attempted to reduce MPC's practical burden. For example, Haddad et al. [13] replaced repeated MPC optimizations with pre-trained control policies for intersection coordination. However, such methods rely on significant training data, additional model complexity, or online computation that can limit real-time deployment. Pham and Ahn [29] proposed a distributed MPC framework based on stochastic decomposition, which splits a large-scale control problem into smaller subproblems that can be solved concurrently. Although this reduces per-node computation time, but it requires low-latency communication and synchronization between nodes, which is chalenging in practice due to communication latency and packet loss. Additionally, model simplification strategies [30], e.g. move-blocking or horizon reduction, rely on dynamic programming and require knowledge of the entire trajectory in advance. Consequently, unexpected traffic fluctuations can significantly reduce control performance as the simplified trajectory no-longer corresponds to real-time conditions. On the other hand, traditional human-driving models are less computationally intensive but unable to predict future states. Therefore, human-based models cannot avoid aggressive braking zones, as schemes only consider the instantaneous state of vehicles to define control input. Furthermore, traditional human-driving schemes have challenges with synchronization issues when transitioning from the idling phase [31, 32].

To address aforementioned limitations, this paper proposes a novel human-based driving model with a time-varying velocity preference parameter, tuned using an optimal trajectory prediction model. A one-time trajectory optimization generates set of optimal velocity profiles and a polynomial braking function prescribes ideal stopping patterns without repeating MPC optimization at each step. Moreover, using the spacing error, a nominal compensation factor provides enhanced synchronization during the transition from idling to the movement of vehicles.

The main contributions of this study are:

(1) Development of a human-based driving model with a time-varying velocity preference parameter for anticipatory intersection driving.

(2) Design of a polynomial braking function fitted to optimal trajectories to replace step-by-step MPC optimization.

(3) Implementation of a safety gap compensation factor for improved synchronization in vehicle start-stop transitions.

(4) Demonstration of improved intersection throughput, fuel efficiency, and other traffic flow metrics through simulation studies [R1C3], [R2C4].

The structure of the paper is as follows: Section 2 describes the methodology, detailing the problem statement, the traditional car-following model, and the proposed optimal driving model. Section 3 presents the simulation results and the key findings. Section 4 concludes the paper, summarizing contributions and providing potential directions for future research.

2 Methodology

The longitudinal traffic flow patterns of a vehicle at a signalized intersection are determined by the state of the PV in the same lane, along with the distance to the intersection and the current signal phase. For simplicity, we focus on singlelane traffic, excluding lane-changing and overtaking maneuvers. This study addresses the longitudinal motion control of vehicles approaching an intersection, assuming that either the driver or an automated system accurately

follows the designated path by steering properly.

The state variables of the host vehicle (HV) are represented by its position x_{hv} and velocity v_{hv}, while the control input is given by its acceleration a_{hv}. The driving task is to determine the control input a_{hv} based on the HV's state variables, along with the state of the PV, which includes its position x_{pv} and velocity v_{pv}. The following section provides a brief overview of a traditional human car-following model for the longitudinal motion control of a HV. Then, we develop a predictive driving system as an extension of this model.

2.1 Traditional Car-Following Scheme

General longitudinal vehicle dynamics can be described using a standard kinematic formulation and can be presented as:

$$
\begin{aligned}
x_n(t+1) &= x_n(t) + v_n(t)\Delta t + 0.5a_n(t)\Delta t^2 \\
v_n(t+1) &= v_n(t) + a_n(t)\Delta t
\end{aligned}
\tag{1}
$$

where, $x_n(t)$, $v_n(t)$, and $a_n(t)$ represent position, velocity, and acceleration at time step t, respectively, with sampling time Δt. These dynamics provide the fundamental framework within which different control strategies are applied, including traditional human driving schemes (HDS) and the proposed predictive scheme.

At first, a brief overview of the traditional HDS is presented. We consider the Intelligent Driver Model (IDM), a widely used framework to replicate human-like driving behavior. The IDM is a time-continuous car-following model that calculates the instantaneous acceleration of HV developed by Treiber et al. [33]. The instantaneous acceleration at time t can be expressed as:

$$
a_{hv}(t) = f_{hds}\left(v_{hv}(t), \Delta v_r(t), \Delta x_r(t), V_d\right)
\tag{2}
$$

where, V_d is the desired speed, $\Delta x_r(t)$ is the actual relative distance to the PV. In case of red signal and no PV ahead, the actual relative distance is considered intersection position X_{red} and is defined as:

$$
\Delta x_r(t) = \begin{cases} X_{red} - x_{hv}(t) - L, & \text{if} x_{pv}(t) > X_{red} \\ x_{pv}(t) - x_{hv}(t) - L, & \text{otherwise} \end{cases}
\tag{3}
$$

where, L is vehicle length, and $\Delta v_r(t)$ is the velocity difference calculated as:

$$
\Delta v_r(t) = \begin{cases} v_{hv}(t), & \text{if} x_{pv}(t) > X_{red} \\ v_{hv}(t) - v_{pv}(t), & \text{otherwise} \end{cases}
\tag{4}
$$

Hence, the function f_{hds} can be defined as:

$$
f_{hds}\left(v_{hv}(t), \Delta v_r(t), \Delta x_r(t), V_d\right) = a\left(1 - \left(\frac{v_{hv}}{V_d}\right)^4 - \left(\frac{D*(v_{hv}, \Delta v_r)^2}{\Delta x_r}\right)\right)
\tag{5}
$$

where, $D^*\left(v_{hv}, \Delta v_r\right)$ is the desired gap from the PV obtained as:

$$
D^*\left(v_{hv}, \Delta v_r\right) = s_0 + v_{hv}T + \frac{v_{hv}\Delta v_r}{2\sqrt{ab}}
\tag{6}
$$

where, s_0, T, a, and b represent the minimum distance, the safe time gap, the maximum acceleration, and the comfortable deceleration rates, respectively. These parameters vary depending on driving style. Specifically, the safe time gap varies within the range $T \in [1, 2]$ s, which often reflects the spectrum from safer to more aggressive driving behavior.

The IDM model ensures collision-free vehicle control in urban traffic. However, despite the computational advantages, IDM focuses on the current states of vehicles, without considering future states, which often leads to suboptimal traffic flow, particularly at signalized intersections. Specifically, the braking behavior of traditional human car-following models at red signals is not energy-efficient. Additionally, the lack of compactness in vehicle movement when transitioning from idling to quick starts at red-to-green signal changes can negatively impact energy consumption and maximum intersection throughput.
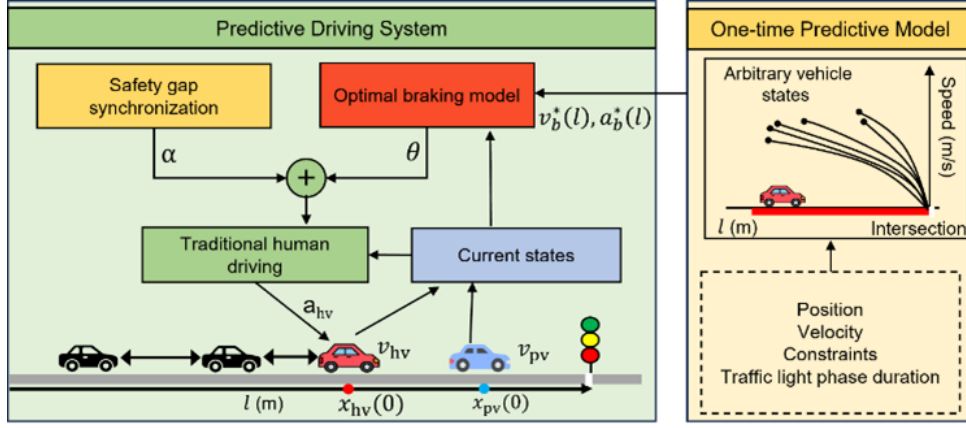
Figure 1. Schematic representation of proposed PDS that integrates predictive braking model and safety gap synchronization into traditional HDS

2.2 Predictive Driving Scheme (PDS)

To address the limitations of HDS, this study introduces a predictive vehicle control system, namely predictive driving scheme (PDS), that integrates driving safety gap synchronization into the IDM and applies an optimal trajectory prediction model for the braking maneuver. As illustrated in Figure 1, the PDS dynamically adjusts the HV's acceleration in response to upcoming traffic signals (e.g., red phase) by a multi-step braking model. Additionally, inter-vehicle spacing is regulated during the steady flow and transitioning from the idling state. Accordingly, the PDS generates a predictive control strategy that mimics naturalistic human driving patterns while enhancing traffic flow efficiency and fuel consumption. The acceleration $a_{hv}(t)$ of the HV at time t is given as:

$$a_{hv}(t) = \theta \left(f_{has}(\cdot) + \alpha \Delta x_r(t) \right) + (1 - \theta) f_{stop} \left(v_{hv}(t), x_{hv}(t) \right) \tag{7}$$

where, α is the compensation coefficient of safety gap regulation, f_{stop} is the optimal stopping trajectory model, and $\theta(t)$ indicates driving mode, which is represented as:

$$\theta(t) = \begin{cases} 1, & \text{if } x_{hv}\left(T_{rem.g}\right) > X_{red} \\ 0, & \text{otherwise} \end{cases} \tag{8}$$

where, $T_{rem.g}$ is the remaining green time. From a modeling perspective, we assume that this information is available to the vehicle in advance through I2V . However, in areas where I2V infrastructure is not available, the remaining green time can be estimated using countdown timers, pedestrian crossing signals, or a yellow signal that indicates a phase transition. Consequently, no signal violation mode at the intersection is given by $\theta(t) = 1$. To avoid aggressive braking rates during the stopping mode ($\theta(t) = 0$), the acceleration of vehicles is dynamically adjusted during the red phase when the vehicle is within a certain distance from the intersection at which drivers can respond to upcoming traffic signals. In such cases, trajectory prediction of vehicles is important to ensure safe and efficient stopping behavior. Therefore, a one-time predictive model (OPM) for vehicle braking over a long horizon T_h is implemented to generate a polynomial braking model.

The objective function of the model is given by:

$$\min_{a_{hv}} J\left(x(0), v(0), a_{hv}\right) = \omega_1 \sum_{t=0}^{T_h} \left(a_{hv}(t)\right)^2 + \omega_2 \sum_{t=0}^{T_h} \left(V_d - v_{hv}(t)\right)^2 \tag{9}$$

Subject to:

$$\begin{aligned} a_{\min} &\leq a_{hv}(t) \leq a_{\max} \\ 0 &\leq v_{hv}(t) \leq V_d \\ x_{hv}\left(T_b\right) &\leq X_{red} \end{aligned} \tag{10}$$

where, ω_1 and ω_2 are weight factors for acceleration and velocity penalties, respectively. Our methodology is inspired by the approach presented in references [28, 34], where a similar polynomial fitting technique was employed to model velocity characteristics based on experimental data. However, our approach is based on solving the optimization problem over the entire signal cycle horizon to generate a set of distinct velocity trajectories for various initial

positions and velocities of the HV [R1C4b]. Then, a typical average velocity curve is obtained using 24 particular stopping patterns as shown in Figure 2. The braking velocity curve $v_{hv}^*(l)$ can be expressed using a polynomial function of the stopping distance l as:

$$v_{hv}^*(l) = \sum_{n=0}^{N} k_n l^n \tag{11}$$

where, k represents the coefficients of the average best-fit polynomial equation, and N is the order of the polynomial, determining the degree of the fitting function. Such a pattern determines the required control acceleration with necessary adjustments instead of repeating the optimization at each step. Specifically, the acceleration of the vehicle precisely following the stopping pattern $v_{hv}^*(l)$ can be determined as:

$$a_{hv}^*(l) = \frac{dv_{hv}^*(l)}{dl}\frac{dl}{dt} = \frac{dv_{hv}^*(l)}{dl}v_{hv}^*(l) \tag{12}$$
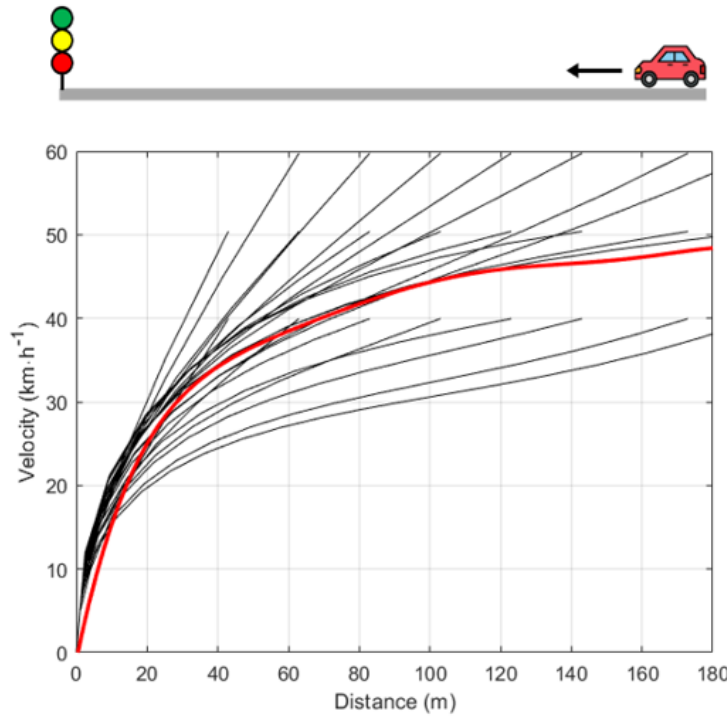

Figure 2. Predicted vehicle stopping patterns along the velocity–stopping distance curve

As shown in Figure 2, the stopping patterns can deviate from the reference velocity $v_{hv}^*(l)$ (e.g., red curve). Depending on current velocity v_{hv}, the acceleration can also vary in Eq. (12) i.e., for $v_{hv} > v_{hv}^*(l)$, vehicle must maneuver with higher braking rate to stop at the same distance l, while for $v_{hv} < v_{hv}^*(l)$, it may stop at the same distance l with a lower braking rate. Consequently, under the assumption that all vehicles stop at the same distance regardless of their initial velocity i.e., the stopping point is referenced to the intersection line and dynamically adjusted in the presence of PVs via the safety-gap compensation term, the general expression for the braking rate is given by [R2C5a]:

$$a_{hv}(l) \approx a_{hv}^*(l)\left(\frac{v_{hv}(l)}{v_{hv}^*(l)}\right)^2 \tag{13}$$

The equation above describes the relationship between acceleration with regard to velocity and stopping distance.

To provide a deeper understanding of the proposed system, Figure 3 presents a system flowchart of PDS. When a vehicle enters the control region, the algorithm first checks for potential red-signal violations. If the vehicle can safely clear the intersection within the remaining green phase, it continues using HDS strategy and simply follows the PV. Otherwise, the PDS control is applied, which uses the polynomial braking function and safety-gap synchronization to plan a smooth deceleration profile. Once the traffic signal transitions to green, the vehicle accelerates to cross the intersection while maintaining safe spacing. This flow illustrates how PDS dynamically switches between predictive and conventional control modes to balance safety, efficiency, and computational simplicity [R1C4a].
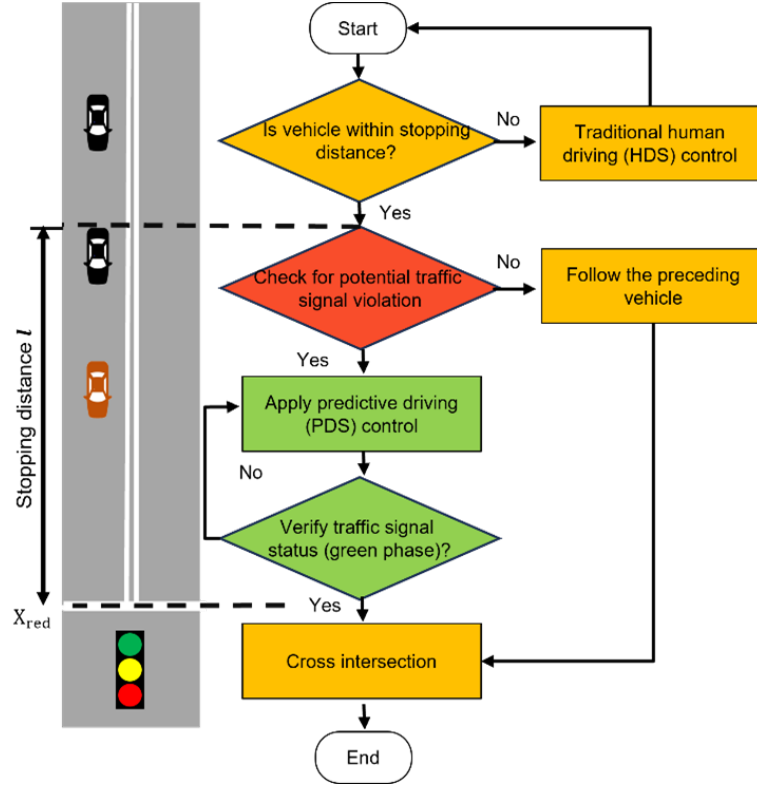
Figure 3. Flowchart of the proposed PDS

2.3 Fuel Consumption Model

The fuel consumption efficiency of the vehicle depends on engine characteristics, such as torque and rotational speed. Additionally, the current speed and acceleration significantly impact fuel usage. In this study, the fuel consumption rate f_v (in mL/s) for a typical vehicle is used as a function of its current velocity v_{hv} and acceleration a_{hv} based on the approach developed in [35]:

$$f_v(v_{hv}, \bar{a}_{hv}) = f_{cruise}(v_{hv}) + f_{dyn}(v_{hv}, \bar{a}_{hv}) \tag{14}$$

where, f_{cruise} is fuel consumption to maintain velocity v_{hv} and f_{dyn} represents additional fuel consumption due to acceleration $\bar{a}_{hv}$ at speed v_{hv}, expressed as:

$$f_{cruise}(v_{hv}) = b_0 + b_1 v_{hv} + b_2 v_{hv}^2 + b_3 v_{hv}^3$$
$$f_{dvn}(v_{hv}, \bar{a}_{hv}) = \bar{a}_{hv}(c_0 + c_1 v_{hv} + c_2 v_{hv}^2) \tag{15}$$

where, b_0, b_1, b_2, b_3, c_0, c_1, and c_2 are approximated parameters for a typical vehicle derived from an engine torque-speed-efficiency map, as described in reference [35], where it has been validated for urban start-stop traffic. Because the model depends on instantaneous acceleration and velocity, it is applicable across different driving scenarios without additional calibration, and was implemented directly in our simulations [R1C4c], [R2C5c]. The acceleration term $\bar{a}_{hv}$ is defined as $\bar{a}_{hv} = a_{hv}$ when $a_{hv} > 0$, and $\bar{a}_{hv} = 0$ when $a_{hv} \leq 0$, under the assumption that no fuel is consumed during highspeed braking. However, once the vehicle slows down to a low speed or comes to a stop, fuel consumption resumes due to engine idling.

3 Results and Discussion

We used a traffic simulator developed in MATLAB to demonstrate the efficiency of the proposed PDS in continuous traffic flow near realistic congested situations in an urban signalized intersection. We evaluated the proposed PDS method in terms of traffic flow, intersection throughput efficiency, and fuel consumption compared to other traditional human car-following schemes, namely the capacity-improved human driving scheme (HDS I) and the safety-improved human driving scheme (HDS II). Accordingly, for HDS I and HDS II, the safe time gaps are defined as $T = 1.2$ s and $T = 1.5$ s. Other simulation parameters for IDM scheme are chosen as $a = 1.5$ m/s^2, $b = 2.5$ m/s^2, $s_0 = 2$ m, $L = 4$ m, and $V_d = 50$ km/h. The simulation time-step is set to $t = 0.5$ s. The compensation factor $\alpha = 0.004$ is applied to compensate synchronization limitations without introducing instability or excessive

speed deviations [R2C5b]. The time horizon for OPM is set to T_h = 30 s with 20 steps and the step-size of Δt = 1.5 s. The velocity and acceleration weight factors are tuned as ω_1 = 15 and ω_2 = 0.4, respectively. We consider N = 6 degree polynomial equation and the coefficients of the polynomial braking velocity equation are obtained as k_6 = -8.290 $\times$ 10^{-12}, k_5 = 5.487 $\times$ 10^{-9}, k_4 = -1.432 $\times$ 10^{-6}, k_3 = 1.889 $\times$ 10^{-4}, k_2 = -1.360 $\times$ 10^{-2}, k_1 = 0.557, and k_0 = 0.0275. The fuel consumption model parameters are b_0 = 0.1569, b_1 = 2.450 $\times$ 10^{-2}, b_2 = -7.415 $\times$ 10^{-4}, b_3 = 5.975 $\times$ 10^{-5}, c_0 = 0.07224, c_1 = 9.681 $\times$ 10^{-2}, and c_2 = 1.075 $\times$ 10^{-3} [35]. Then, the microscopic traffic simulations are conducted to evaluate the performance of the proposed PDS scheme.

3.1 Evaluation of Acceleration and Braking Behavior at Intersection

Firstly, we analyze the acceleration and braking behavior among HDS I, OPM, and the proposed PDS method. The purpose of this analysis is to evaluate how each method responds to intersection constraints during the red signal phase. In this evaluation, it is assumed that the HV starts at different distances and velocity profiles while approaching an intersection with red signal on traffic light. Accordingly, a grid of initial conditions is constructed by varying the vehicle velocity between 42 km/h and 50 km/h and the distance to the intersection from 80 m to 200 m. At each grid point, the acceleration from each control strategy is collected to generate a corresponding heatmap.

Figure 4 presents a comparative analysis of vehicle acceleration and braking behavior under varying initial conditions of distance and velocity. Each cell in the heatmap represents the resulting acceleration for a given initial condition. Warmer colors (e.g., red or yellow) indicate positive or near-zero acceleration, while cooler colors (e.g., dark blue) reflect strong deceleration, corresponding to aggressive braking behavior. Figure 4b shows that OPM employs predictive optimization over a long horizon, leading to gradual braking behavior when the distance to the intersection is short or the vehicle velocity is high. In contrast, Figure 4a HDS I demonstrates the most aggressive deceleration, as reflected in relatively abrupt and late braking patterns. The proposed model (Figure 4c) dynamically adjusts acceleration based on the polynomial braking velocity curve and inter-vehicle coordination, resulting in smoother deceleration patterns with reduced braking intensity in comparison to HDS I. In long-distance and lower-velocity conditions, OPM demonstrates low acceleration, while HDS I presents the highest acceleration patterns. Alternatively, PDS performs comparable dynamics to OPM. Compared to HDS I, our proposed approach significantly reduces sudden braking events, leading to improved passenger comfort while maintaining lower computational complexity than MPC. By balancing efficiency and smooth vehicle operation, the proposed model offers a practical alternative for real-time traffic optimization at signalized intersections.
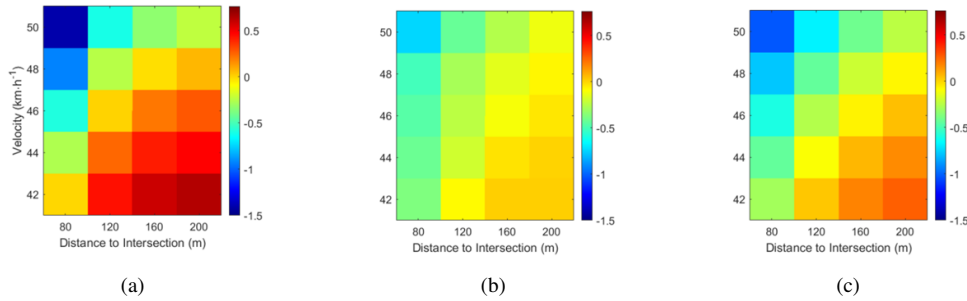

Figure 4. Acceleration and braking behavior of the HV: (a) HDS I; (b) OPM; (c) PDS

3.2 Evaluation of Proposed System in Continuous Traffic Flow

Next, we evaluate the performance of the proposed PDS in continuous near-congested traffic conditions at signalized intersections and compare it to the HDS I and HDS II methods. A single-lane road with one intersection positioned at 400 m is considered. The total traffic light cycle has a 60 s duration, split evenly between green (including the final 3 s of yellow signal) and red phases. Initially, every scheme had the same set of traffic and signal settings for fair comparison. Specifically, at 0 s, the traffic light has a green signal, and vehicles approach the intersection at a standard speed limit of 50 km/h, with an approximately 780 veh/hour flow rate, which is obtained by randomly generating inter-vehicle spacing to reflect stochastic traffic arrivals. As the traffic light changes to red, vehicles decelerate and stop at the intersection. Figure 5 illustrates the vehicle's position, speed, and acceleration profiles over 300 s for each scheme.

It is found that HDS I has 12 vehicles per cycle intersection capacity, while 11 vehicles can successfully pass the intersection in HDS II as depicted in Figure 5a and 5b. On the contrary, the proposed PDS has the highest intersection clearance rate per cycle with 13 vehicles, as shown in Figure 5c. Moreover, it can be observed that one and two vehicles per cycle fail to cross the intersection in HDS I and HDS II, respectively, whilst all vehicles successfully clear

the intersection in the proposed PDS. Consequently, HDS I and HDS II generate longer queue formations leading to spill-back congestion, which results in increased fuel consumption and traffic delays. In contrast, the proposed PDS improves traffic flow by increasing flow synchronization and reducing starting lost time at the intersection. As a result of the improvement of effective green time, PDS significantly improves the intersection transit time under dense traffic flow conditions.
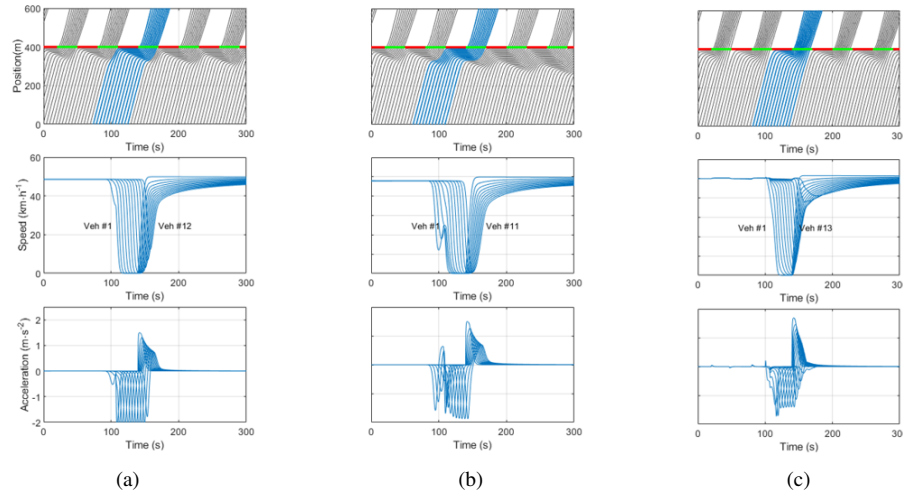

Figure 5. State profiles of continuous traffic over 300 s with one signalized intersection. The sub-plots illustrate the vehicle's position (top), speed (middle), and acceleration (bottom) profiles under near-congested traffic conditions: (a) HDS I; (b) HDS II; (c) PDS

Figure 5 (middle and bottom) compares the velocity and acceleration profiles for successive vehicles at the intersection under different schemes. According to velocity profiles, both HDS methods perform similarly due to the fundamental principles of the IDM model. In both schemes, vehicles decelerate at a higher rate compared to PDS and reach a complete stop at the intersection during the red signal phase. In contrast, in the proposed PDS, vehicles experience a more gradual slowdown process while approaching the intersection at the red signal. Additionally, the velocity prediction model enables vehicles to avoid a complete stop at the intersection. Furthermore, vehicles using PDS demonstrate faster speeding up than the HDS I and HDS II, while still avoiding collisions. Consequently, quick speeding up enables efficient clearance of traffic congestion and improves overall intersection throughput. It can be seen from the acceleration profiles that in HDS I and HDS II, vehicles experience aggressive braking during the stopping phase, whereas PDS decelerate slowly according to the predictive velocity curve. Therefore, decreasing the deceleration magnitude can comparatively improve not only fuel consumption but also traffic flow efficiency by avoiding abrupt stop-and-go behavior.

Figure 6a demonstrates the queue density within 150 meters of the intersection, measured at the beginning of each green phase over 10 minutes for HDS I, HDS II, and PDS. The queue density, defined as the number of vehicles approaching a stopping condition $v_{hv} < 2$ m/s, has a distinct pattern across all schemes. Specifically, the HDS II scheme consistently shows the highest queue density, starting at 8 vehicles at 60 seconds and increasing steadily to 20 vehicles by 600 seconds. Conversely, the HDS I scheme presents moderate queue density, ranging between 8 and 14 vehicles, with a comparatively slower growth rate than HDS I. The PDS maintains a minimal queue density, ranging between 8 and 10 vehicles, indicating better traffic flow and reduced congestion at the intersection. Additionally, Figure 6b illustrates the average fuel consumption rate for the vehicles in the queue throughout the range of 150–450 m, corresponding to the intersection transition region, where notable speed variations can be observed. The findings are directly related to queue density length. PDS scheme consistently achieves the highest fuel consumption rate in comparison to HDS I and HDS II. Consequently, it might be considered that these results emphasize the effectiveness of the PDS in reducing queue formation, which is essential for enhancing intersection throughput, minimizing delays, and increasing the fuel consumption rate.

Table 1 presents a performance comparison of HDS I, HDS II, and the proposed PDS schemes on essential traffic metrics: fuel consumption, acceleration/deceleration dynamics, and intersection throughput. The evaluation covers region 150 m before and after the intersection where speed variations occur due to stop-and-go situations. Along with safety improvements, HDS II demonstrates the lowest fuel efficiency, with approximately a 20.08 km/L rate, due to aggressive deceleration and increased queue formation, which lead to greater fuel consumption. HDS I shows a moderate 7.93% improvement with a fuel consumption rate of around 21.81 km/L. Conversely, the proposed PDS achieves the highest fuel consumption efficiency, with a rate of around 24.21 km/L, reflecting a 17.06% enhancement

over the THD II scheme. The PDS method minimizes excessive braking and acceleration, leading to reduced fuel consumption compared to HDS I and HDS II. Additionally, the PDS scheme demonstrates smoother driving patterns, with the lowest average deceleration rates at -1.13 m/s^2, in contrast to -1.41 m/s^2 for THD II and -1.62 m/s^2 for THD I. The mean maximum acceleration for PDS is 1.21 m/s^2, which indicates efficient intersection throughput. Consequently, the aforementioned improvements result in reduced congestion and shorter queue lengths, contributing to overall traffic flow improvement.
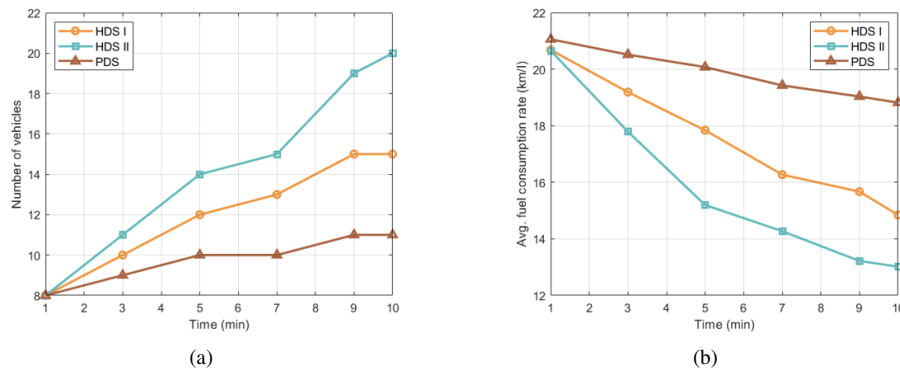

Figure 6. Evaluation of of HDS I, HDS II, and PDS vehicles at the intersection over 10 minutes: (a) Queue density; (b) Average fuel consumption rate

Table 1. Performance evaluation of HDS I, HDS II, and proposed PDS methods

	HDS I	HDS II	PDS
Average fuel consumption rate (km/L)	21.81	20.08	24.21
Improvement with respect to HDS II	+7.93%		+17.06%
Mean maximum acceleration (m/s^2)	1.04	1.02	1.21
Mean maximum deceleration (m/s^2)	-1.62	-1.41	-1.13
Observed throughput per cycle (vehicles)	12	11	13
Throughput per hour (vehicles)	720	660	780

3.3 Evaluation of Proposed System at Different Penetration Rates

Finally, the overall performance of the proposed system is analyzed using mixed traffic conditions with varying penetration rates (0%, 25%, 50%, 75%, 100%) of PDS-equipped vehicles 5 independent times with randomized vehicle arrivals. Figure 7 illustrates the average traffic performance for a 10-minute simulated period. Each subplot provides means and 95% confidence intervals of specific metrics, namely average speed, fuel consumption efficiency, intersection throughput, and total idle time, in varying penetration rates. The results indicate that with the increase of PDS-driven vehicles, the overall performance of the traffic flow significantly increases. As shown, intersection throughput increases by approximately 12%, total idling time reduces nearly by 50%, and fuel efficiency improves by about 21% compared with the baseline case at 0% penetration rate [R2C6]. It can be said that the PDS has the potential to improve traffic flow efficiency and reduce energy consumption, making it suitable for mixed-traffic urban environments. The ability to maintain better performance under different penetration rates emphasizes its effectiveness in managing real-world traffic conditions.

3.4 Discussion

Overall, the proposed PDS demonstrates effectiveness in maintaining smooth speed transitions during stop-and-go events. It follows the stopping phase velocity curve to effectively minimize aggressive braking zones, resulting in significant enhancements in fuel consumption efficiency. In addition, intersection clearance time is reduced while maintaining a safety gap synchronization. These improvements are achieved without compromising computational efficiency since the PDS scheme maintains lower computational complexity relative to conventional MPC-based algorithms.

However, several limitations should be acknowledged. First, the current simulations assume a single-lane road with homogeneous vehicle characteristics and consistent driver behavior. In practice, urban traffic involves mixed fleets (e.g., heavy trucks, buses, and electric vehicles) and diverse driving styles, which could influence braking and

synchronization characteristics. Therefore, future work should extend the model to multi-lane scenarios that include lane-change, overtaking, and merging decisions, and evaluate performance within larger and more complex road networks.
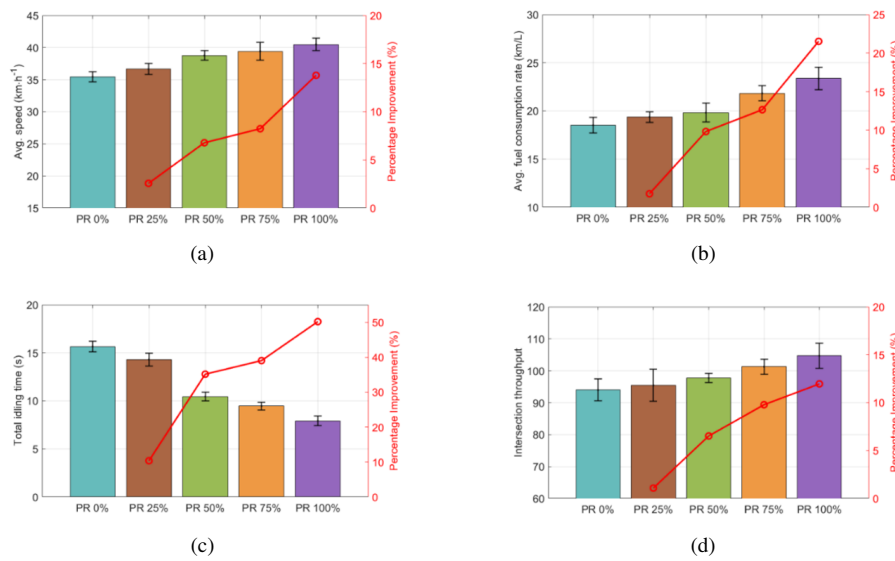

Figure 7. Traffic flow performance at varied penetration rates. The red curve indicates the percentage improvement in performance metrics relative to the baseline condition at PR 0%: (a) Average speed; (b) Average fuel consumption rate; (c) Total idling time; (d) Intersection throughput

Secondly, the method relies on I2V communication or signal-phase estimation, which in real deployments may be subject to latency, packet loss, or sensor noise. In this study, the system needs to receive traffic signal information only once per approach, which requires comparatively low latency and makes the communication less critical. In addition, we evaluated computation time and confirmed that PDS executes in only 2 ms, which is approximately $25\times$ faster than MPC for equivalent scenarios, demonstrating its suitability for real-time implementation without compromising performance. While preliminary simulations assumed ideal communication, assessing PDS performance under realistic delays and imperfect signal information is essential.

Finally, this study focused on steady inflow conditions at a single fixed-cycle intersection. Additional sensitivity analyses, such as varying signal timings and intersection geometries, will help to further validate robustness. However, in our preliminary investigations, even when traffic flow is below capacity, the PDS still provides benefits by smoothing acceleration and deceleration, which reduces extra fuel consumption and improves traffic flow efficiency. Since the focus of this paper is on critical scenarios, where both capacity and performance improvement are essential, we have not included these low-capacity results in the paper for brevity. As part of our future research, we plan to link the PDS with adaptive traffic light control and evaluate its broader effects on traffic efficiency across multiple coordinated intersections [R1C5], [R2C6].

4 Conclusions

This study introduces a PDS that integrates optimal trajectory approximation and safety-gap compensation within an extended IDM to enhance traffic flow and fuel efficiency at signalized intersections. The proposed PDS ensures safe driving by retaining the collision-free feature of IDM and can make real-time optimal decisions with negligible computation time compared to the control cycle length, thereby facilitating real-time operation. Microscopic simulations under near-congested urban conditions demonstrated that PDS can enhance intersection throughput by approximately 12% and increase fuel efficiency by about 21% compared to a zero-penetration baseline model, which represents a typical human driver model. These results demonstrate that anticipatory braking with real-time computation can achieve performance comparable to more computationally intensive MPC methods.

In this study, focusing solely on vehicle control evaluation, the simulations assumed homogeneous vehicle types and consistent driver behavior, which may not fully reflect the real-world variability. Moreover, the method currently relies on I2V communication in an ideal communication environment, which is still under development. Future research will evaluate PDS in mixed traffic environments with varying vehicle classes and human-driver variability, incorporate emergency braking and pedestrian crossing scenarios, and quantify robustness under sensor noise and communication latency [R1C6], [R2C7].

Author Contributions

Funding

Data Availability

The data used to support the research findings are available from the corresponding author upon request.

Conflicts of Interest

The authors declare no conflict of interest.

References

[1] A. Ait Ouallane, A. Bakali, A. Bahnasse, S. Broumi, and M. Talea, "Fusion of engineering insights and emerging trends: Intelligent urban traffic management system," *Inform. Fusion*, vol. 88, pp. 218–248, 2022. https://doi.org/10.1016/j.inffus.2022.07.020

[2] T. Jayson, A. S. M. Bakibillah, C. P. Tan, M. A. S. Kamal, V. Monn, and J. I. Imura, "Electric vehicle eco-driving strategy at signalized intersections based on optimal energy consumption," *J. Environ. Manage.*, vol. 368, p. 122245, 2024. https://doi.org/10.1016/j.jenvman.2024.122245

[3] S. Alshayeb, A. Stevanovic, and J. R. Effinger, "Investigating impacts of various operational conditions on fuel consumption and stop penalty at signalized intersections," *Int. J. Transp. Sci. Technol.*, vol. 11, no. 4, pp. 690–710, 2022. https://doi.org/10.1016/j.ijtst.2021.09.005

[4] W. Yue, C. Li, Y. Chen, P. Duan, and G. Mao, "What is the root cause of congestion in urban traffic networks: Road infrastructure or signal control?" *IEEE Trans. Intell. Transp. Syst.*, vol. 23, no. 7, pp. 8662–8679, 2021. https://doi.org/10.1109/TITS.2021.3085021

[5] H. Xia, K. Boriboonsomsin, F. Schweizer, A. Winckler, K. Zhou, W. B. Zhang, and M. Barth, "Field operational testing of eco-approach technology at a fixed-time signalized intersection," in *2012 15th International IEEE Conference on Intelligent Transportation Systems, Anchorage, USA*, 2012, p. 6338888. https://doi.org/10.1109/ITSC.2012.6338888

[6] P. B. Mirchandani and N. Zou, "Queuing models for analysis of traffic adaptive signal control," *IEEE Trans. Intell. Transp. Syst.*, vol. 8, no. 1, pp. 50–59, 2007. https://doi.org/10.1109/TITS.2006.888619

[7] H. X. Liu, X. Wu, W. Ma, and H. Hu, "Real-time queue length estimation for congested signalized intersections," *Transp. Res. Part C: Emerg. Technol.*, vol. 17, no. 4, pp. 412–427, 2009. https://doi.org/10.1016/j.trc.2009.02.003

[8] B. Asadi and A. Vahidi, "Predictive cruise control: Utilizing upcoming traffic signal information for improving fuel economy and reducing trip time," *IEEE Trans. Control Syst. Technol.*, vol. 19, no. 3, pp. 707–714, 2010. https://doi.org/10.1109/TCST.2010.2047860

[9] Z. Nie and H. Farzaneh, "Real-time dynamic predictive cruise control for enhancing eco-driving of electric vehicles, considering traffic constraints and signal phase and timing (SPaT) information, using artificial-neural-network-based energy consumption model," *Energy*, vol. 241, p. 122888, 2022. https://doi.org/10.1016/j.energy.2021.122888

[10] H. Wang, M. Zhu, W. Hong, C. Wang, G. Tao, and Y. Wang, "Optimizing signal timing control for large urban traffic networks using an adaptive linear quadratic regulator control strategy," *IEEE Trans. Intell. Transp. Syst.*, vol. 23, no. 1, pp. 333–343, 2020. https://doi.org/10.1109/TITS.2020.3010725

[11] Z. Yin, T. Liu, C. Wang, H. Wang, and Z. P. Jiang, "Reducing urban traffic congestion using deep learning and model predictive control," *IEEE Trans. Neural Netw. Learn. Syst.*, vol. 35, no. 9, pp. 12 760–12 771, 2023. https://doi.org/10.1109/TNNLS.2023.3264709

[12] A. S. M. Bakibillah, M. A. S. Kamal, C. P. Tan, T. Hayakawa, and J. I. Imura, "Event-driven stochastic eco-driving strategy at signalized intersections from self-driving data," *IEEE Trans. Veh. Technol.*, vol. 68, no. 9, pp. 8557–8569, 2019. https://doi.org/10.1109/TVT.2019.2931519

[13] T. A. Haddad, D. Hedjazi, and S. Aouag, "A deep reinforcement learning-based cooperative approach for multi-intersection traffic signal control," *Eng. Appl. Artif. Intell.*, vol. 114, p. 105019, 2022. https://doi.org/10.1016/j.engappai.2022.105019

[14] G. J. L. Naus, R. P. A. Vugts, J. Ploeg, M. J. G. van De Molengraft, and M. Steinbuch, "String-stable CACC design and experimental validation: A frequency-domain approach," *IEEE Trans. Veh. Technol.*, vol. 59, no. 9, pp. 4268–4279, 2010. https://doi.org/10.1109/TVT.2010.2076320

[15] I. A. Ntousakis, I. K. Nikolos, and M. Papageorgiou, "On microscopic modelling of adaptive cruise control systems," *Transp. Res. Procedia*, vol. 6, pp. 111–127, 2015. https://doi.org/10.1016/j.trpro.2015.03.010

[16] S. Moon, I. Moon, and K. Yi, "Design, tuning, and evaluation of a full-range adaptive cruise control system with collision avoidance," *Control Eng. Pract.*, vol. 17, no. 4, pp. 442–455, 2009. https://doi.org/10.1016/j.conengprac.2008.09.006

[17] D. Manolis, A. Spiliopoulou, F. Vandorou, and M. Papageorgiou, "Real time adaptive cruise control strategy for motorways," *Transportation Res. Part C: Emerg. Technol.*, vol. 115, p. 102617, 2020. https://doi.org/10.1016/j.trc.2020.102617

[18] V. Milanés and S. E. Shladover, "Modeling cooperative and autonomous adaptive cruise control dynamic responses using experimental data," *Transp. Res. C: Emerg. Technol.*, vol. 48, pp. 285–300, 2014. https://doi.org/10.1016/j.trc.2014.09.001

[19] A. Talebpour and H. S. Mahmassani, "Influence of connected and autonomous vehicles on traffic flow stability and throughput," *Transp. Res. C: Emerg. Technol.*, vol. 71, pp. 143–163, 2016. https://doi.org/10.1016/j.trc.2016.07.007

[20] C. Lu, J. Dong, L. Hu, and C. Liu, "An ecological adaptive cruise control for mixed traffic and its stabilization effect," *IEEE Access*, vol. 7, pp. 81 246–81 256, 2019. https://doi.org/10.1109/ACCESS.2019.2923741

[21] E. Papapanagiotou and F. Busch, "Extended observer for urban traffic control based on limited measurements from connected vehicles," *IEEE Trans. Intelligent Transp. Systems*, vol. 21, no. 4, pp. 1664–1676, 2019. https://doi.org/10.1109/TITS.2019.2939904

[22] I. H. Zohdy and H. A. Rakha, "Intersection management via vehicle connectivity: The intersection cooperative adaptive cruise control system concept," *J. Intell. Transp. Syst.*, vol. 20, no. 1, pp. 17–32, 2016. https://doi.org/10.1080/15472450.2014.889918

[23] L. Xiao, M. Wang, W. Schakel, and B. van Arem, "Unravelling effects of cooperative adaptive cruise control deactivation on traffic flow characteristics at merging bottlenecks," *Transp. Res. C: Emerg. Technol.*, vol. 96, pp. 380–397, 2018. https://doi.org/10.1016/j.trc.2018.10.008

[24] Y. Liu, W. Wang, X. Hua, and S. Wang, "Safety analysis of a modified cooperative adaptive cruise control algorithm accounting for communication delay," *Sustainability*, vol. 12, no. 18, p. 7568, 2020. https://doi.org/10.3390/su12187568

[25] Z. Li, Y. Zhou, D. Chen, and Y. Zhang, "Disturbances and safety analysis of linear adaptive cruise control for cut-in scenarios: A theoretical framework," *Transp. Res. C: Emerg. Technol.*, vol. 168, p. 104576, 2024. https://doi.org/10.1016/j.trc.2024.104576

[26] A. S. M. Bakibillah, M. Hasan, M. M. Rahman, and M. A. S. Kamal, "Predictive car-following scheme for improving traffic flows on urban road networks," *Control Theory Tech.*, vol. 17, pp. 325–334, 2019. https://doi.org/10.1007/s11768-019-9144-z

[27] K. Yu, J. Yang, and D. Yamaguchi, "Model predictive control for hybrid vehicle ecological driving using traffic signal and road slope information," *Control Theory Tech.*, vol. 13, pp. 17–28, 2015. https://doi.org/10.1007/s11768-015-4058-x

[28] M. A. S. Kamal, M. Mukai, J. Murata, and T. Kawabe, "Ecological driving based on preceding vehicle prediction using MPC," *IFAC Proc. Vol.*, vol. 44, no. 1, pp. 3843–3848, 2011. https://doi.org/10.3182/20110828-6-IT-1002.02748

[29] V. H. Pham and H. S. Ahn, "Distributed stochastic MPC traffic signal control for urban networks," *IEEE Trans. Intell. Transp. Syst.*, vol. 24, no. 8, pp. 8079–8096, 2023. https://doi.org/10.1109/TITS.2023.3262580

[30] L. Koch, T. Brinkmann, M. Wegener, K. Badalian, and J. Andert, "Adaptive traffic light control with deep reinforcement learning: An evaluation of traffic flow and energy consumption," *IEEE Trans. Intell. Transp. Syst.*, vol. 24, no. 12, pp. 15 066–15 076, 2023. https://doi.org/10.1109/TITS.2023.3305548

[31] D. L. Fisher, M. Lohrenz, D. Moore, E. D. Nadler, and J. K. Pollard, "Humans and intelligent vehicles: The hope, the help, and the harm," *IEEE Trans. Intell. Veh.*, vol. 1, no. 1, pp. 56–67, 2016. https://doi.org/10.1109/TIV.2016.2555626

[32] M. H. Martens and A. P. van den Beukel, "The road to automated driving: Dual mode and human factors considerations," in *16th International IEEE Conference on Intelligent Transportation Systems (ITSC 2013), The Hague, Netherlands*, 2013, pp. 2262–2267. https://doi.org/10.1109/ITSC.2013.6728564

[33] M. Treiber, A. Hennecke, and D. Helbing, "Congested traffic states in empirical observations and microscopic simulations," *Phys. Rev. E*, vol. 62, p. 1805, 2000. https://doi.org/10.1103/PhysRevE.62.1805

[34] M. A. S. Kamal, M. Mukai, J. Murata, and T. Kawabe, "Model predictive control of vehicles on urban roads for improved fuel economy," *IEEE Trans. Control Syst. Technol.*, vol. 21, no. 3, pp. 831–841, 2012. https://doi.org/10.1109/TCST.2012.2198478

[35] M. A. S. Kamal, M. Mukai, J. Murata, and T. Kawabe, "Ecological vehicle control on roads with up-down slopes," *IEEE Trans. Intell. Transp. Syst.*, vol. 12, no. 3, pp. 783–794, 2011. https://doi.org/10.1109/TITS.2011.2112648